Applied Mathematics, Modeling and Computer Simulation
C.-H. Chen et al. (Eds.)

doi:10.3233/ATDE231018

Research on Nonlinear Trajectory Tracking Control Method for Autonomous Vehicles

Jinli XIE [a,1]
[a] *Chongqing Metropolitan College of Science and Technology, Chongqing, China*

Abstract. The trajectory tracking model of autonomous vehicles is usually simplified to a linear model, and then the matching controller is designed. However, the simplification process of the model requires a lot of assumptions, which are difficult to be established. For this reason, a nonlinear trajectory tracking control method is proposed. Firstly, a system error dynamics model is established based on the vehicle kinematics model and dynamics model, and the steady state control law for the vehicle trajectory tracking control is deduced on this basis. Then, the compensation control law based on the vehicle lateral displacement error is further designed to improve the system's anti-interference. The effectiveness of the proposed control method is verified by comparing with the commonly used controllers for vehicle trajectory tracking, and the results show that the control accuracy and convergence speed of the proposed control method are effectively improved.

Keywords. intelligent vehicle; trajectory tracking; reliability; steady-state control; transient control

1. Introduction

Intelligent driving technology can effectively improve the efficiency of traffic travelling and vehicle driving safety, and has become the development trend of automotive technology. Trajectory tracking control, as one of the core technologies of automatic driving, is directly related to vehicle driving safety and driving comfort, and therefore is one of the key research areas of automatic driving technology.

Currently, trajectory tracking control methods mainly include three main categories: model-free trajectory tracking control methods, linear model-based trajectory tracking control methods and nonlinear model-based trajectory tracking control methods. Model-free trajectory tracking control methods include such as neural network control [1-2], model-free adaptive iterative learning control [3], fuzzy control [3-4], game methods [5], model-free adaptive control [6-7], reinforcement learning [8], and so on. The model-free trajectory tracking control method is a rule-based approach that requires a large amount of experimental data as a basis for design, which makes the design of the controller very difficult. The design process of linear model-based trajectory tracking control methods simplifies and approximates the model, which greatly simplifies the design of the controller and reduces the arithmetic requirements. Therefore are currently commonly used control methods such as Pure Pursuit trajectory

1 Corresponding Author, Jinli XIE, Chongqing Metropolitan College of Science and Technology, Chongqing, China; E-mail: xiejinli2477@126.com.

tracking control [9], LQR control [10], H∞ control [11], Model Predictive Control(MPC) [12-13], Linear Matrix Inequality methods [14], and Self-Antithetic Control [15].

Unlike linear trajectory tracking control methods, nonlinear trajectory tracking control methods are designed without linearization and oversimplification of the model, e.g. nonlinear model predictive control(NMPC) [16-19], sliding mode control(SMC) [20-22], and backstepping control [23-24]. NMPC can be used to deal with control problems of nonlinear systems with high control accuracy. NMPC can well solve the nonlinear control problem of coupling class, but NMPC designed with dynamic feedback method has high state quantity dimension and poor real-time performance. SMC can be used for the control of nonlinear systems with input and state constraints as well as nonlinear systems with input constraints. The control method is robust and resistant to interference, but is prone to high-frequency jitter. To solve the jitter problem, more complex convergence laws need to be designed or combined with fuzzy strategies and neural networks [25]. Backstepping control is also a commonly used nonlinear control method, which is often used to solve control problems for nonlinear systems with incomplete constraints. The backstepping control design process is simple and the control accuracy is high, but it will produce over-parameterization problems as the order of the system rises, so it is often used in combination with neural network control, fuzzy control and sliding mode control. Beyond that, some other robust control methods have been proposed by some scholars. For example, Chen et al,. [26-27] proposed a nonlinear robust control method for underdriven systems with non-matching uncertainty, which can deal with system uncertainty with good robustness, but the controller design needs to convert the system dynamics equations into a unique form, which is less practical. All of the above nonlinear control methods can effectively improve the robustness and anti-interference ability of the vehicle trajectory tracking control system to ensure the trajectory tracking performance of the vehicle, but due to the complexity of the algorithms, high arithmetic power demand and bad real-time performance, they are rarely used in practical applications. Beyond that, all the above three types of trajectory tracking control are in terms of vehicle state indicator state quantities such as lateral displacement error, heading angle error and yaw rate. However, limited by the current sensing technology, the parameters collected through the sensors (lateral displacement, heading angle and yaw rate, etc.) are easily interfered with, and some of the parameters cannot be obtained directly, but need to be obtained indirectly through estimation (center of mass lateral deflection angle, lateral velocity, etc.). When there is a large error in the data collected by the sensor, it can lead to a degradation in the performance of trajectory tracking and even affect vehicle safety.

To improve the reliability and control accuracy of the trajectory tracking method, a trajectory tracking control method (S&T) based on the error dynamics model is proposed, which consists of two parts, steady state control law and transient control law. The steady state control law was firstly derived from the vehicle kinematics and error dynamics models. Then the error dynamics model is corrected by considering the vehicle trajectory tracking error, and the transient control law is designed based on the control error. Finally, the effectiveness of the proposed method is verified by simulation. The results show that the S&T trajectory tracking control method can effectively improve the control accuracy.

2. Mathematical model

2.1. Kinematic Model

In order to reflect the relative position relationship between the vehicle and the reference trajectory during trajectory tracking, the vehicle trajectory tracking model shown in Figure 1 is established. The local coordinate system *xoy* and the inertial coordinate system *XOY* are defined, and the vehicle will generate heading angle error and lateral position error when tracking the intended trajectory.

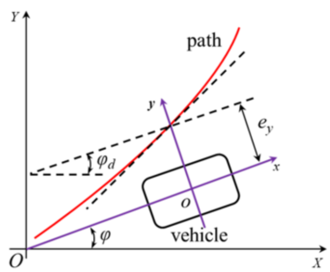

Figure 1. Trajectory tracking error model

The heading angle error is the difference between the vehicle heading angle and the ideal heading angle: $e_\varphi = \varphi - \varphi_d$.Generally, the desired heading angular velocity $\dot{\varphi}_d$ can be expressed as the product of the desired trajectory curvature ρ and the longitudinal velocity v_x:

$$\dot{\varphi}_d = v_x \rho \tag{1}$$

The first order derivative of e_φ can be expressed as:

$$\dot{e}_\varphi = \dot{\varphi} - v_x \rho \tag{2}$$

The first order derivative of the vehicle's lateral position error e_y is:

$$\dot{e}_y = v_y \cos e_\varphi + v_x \sin e_\varphi \tag{3}$$

where v_y is the vehicle lateral velocity.

The heading angle error during trajectory tracking is generally small, and taking into account modelling and sensor measurement errors, $\dot{e}_y$, $\ddot{e}_y$and $\dot{e}_\varphi$ can be further expressed as:

$$\begin{cases} \dot{e}_y = v_y + v_x e_\varphi + d_1 \\ \ddot{e}_y = \dot{v}_y + v_x \dot{\varphi} - v_x^2 \rho + d_2 \\ \dot{e}_\varphi = \dot{\varphi} - v_x \rho + d_3 \end{cases} \tag{4}$$

where d_1, $d_2$and d_3 are errors due to mathematical modelling and sensor measurements.

2.2. Dynamical Model

The forces in the lateral and yaw directions of the vehicle are analysed in the local and inertial coordinate systems *xoy* and *XOY*, as shown in Figure 2.

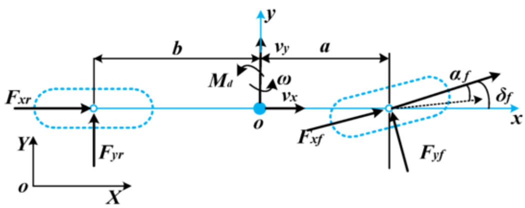

Figure 2. Convolution kernel design for insulator cracks

The dynamic equations of the vehicle in lateral and yaw direction can be expressed as:

$$\begin{cases} F_{yf}\cos\delta_f + F_{yr} + F_d = m\left(\dot{v}_y + v_x\omega\right) \\ aF_{yf}\cos\delta_f - bF_{yr} + M_d = I_z\dot{\omega} \end{cases} \tag{5}$$

where δ_f is the angle of rotation of the front wheel, F_{yf} and F_{yr} are the lateral deflection forces of the front and rear wheels, ω is the angular velocity of the yaw direction, whose magnitude is approximated by $\dot{\varphi}$, I_z is the rotational inertia around the z-axis, F_d is the other external disturbance force, M_d is the other external disturbance moment.

Assuming a constant vehicle longitudinal speed and neglecting the lateral load transfer, and also in the case that both the front wheel turning angle δ_f and the tyre lateral deflection angle are small, according to the Pacejka tyre model[28], F_{yf} and F_{yr} can be simplified as:

$$\begin{cases} F_{yf} = C_f\alpha_f \\ F_{yr} = C_r\alpha_r \end{cases} \tag{6}$$

where C_f and C_r are the front and rear wheel lateral deflection stiffnesses respectively.

In Eq. (6), the front and rear wheel side deflections are:

$$\begin{cases} \alpha_f = -\tan^{-1}\left(\dfrac{v_y + a\omega}{v_x}\right) + \delta_f \\ \alpha_r = -\tan^{-1}\left(\dfrac{v_y - b\omega}{v_x}\right) \end{cases} \tag{7}$$

where a, b are the distances from the center of mass of the vehicle to the front and rear axles respectively.

Bringing Eq. (6) and Eq. (7) into Eq. (4), since δ_f is small, $\cos\delta_f \approx 1$ can be obtained:

$$\begin{cases} \dot{v}_y = -\dfrac{C_f}{m}\tan^{-1}\left(\dfrac{v_y + a\omega}{v_x}\right) - \dfrac{C_r}{m}\tan^{-1}\left(\dfrac{v_y - b\omega}{v_x}\right) - v_x\omega + \dfrac{F_d}{m} + \dfrac{C_f}{m}\delta_f \\ \dot{\omega} = -\dfrac{aC_f}{I_z}\tan^{-1}\left(\dfrac{v_y + a\omega}{v_x}\right) + \dfrac{bC_r}{I_z}\tan^{-1}\left(\dfrac{v_y - b\omega}{v_x}\right) + \dfrac{M_d}{I_z} + \dfrac{aC_f}{I_z}\delta_f \end{cases} \tag{8}$$

Disregarding external disturbances, Eq. (8) can be further converted to:

$$\begin{cases} \dot{v}_y = -\dfrac{C_f}{m}\tan^{-1}\left(\dfrac{v_y + a\omega}{v_x}\right) - \dfrac{C_r}{m}\tan^{-1}\left(\dfrac{v_y - b\omega}{v_x}\right) - v_x\omega + \dfrac{C_f}{m}\delta_f \\ \dot{\omega} = -\dfrac{aC_f}{I_z}\tan^{-1}\left(\dfrac{v_y + a\omega}{v_x}\right) + \dfrac{bC_r}{I_z}\tan^{-1}\left(\dfrac{v_y - b\omega}{v_x}\right) + \dfrac{aC_f}{I_z}\delta_f \end{cases} \tag{9}$$

3. Controller Design

The goal of vehicle trajectory tracking is to make the error between the lateral displacement of the vehicle and the reference trajectory zero, so according to Eq. (4), the controller design goal is determined as follows: to make e_y converge quickly by designing a reasonable control rate.

3.1. Steady-state Control

In order to design a control rate that satisfies the objective, the stable equilibrium point of the system's dynamics equation is first determined and used to calculate the system's error dynamics equation.

Ideal values for each metric can be obtained based on vehicle dynamics [29]:

$$\begin{cases} v_{yd} = bv_x\rho + v_x\tan\left(\dfrac{-mav_x^2}{2C_r(a+b)}\rho\right) \\ \omega_d = v_x\rho \\ \delta_{fd} = \dfrac{v_x^2}{\dfrac{2aC_r}{mb} + \dfrac{2C_r}{m}}\rho \end{cases} \tag{10}$$

The error dynamics model of the system can be obtained from Eq. (9) and Eq. (10):

$$\begin{cases} \dot{v}_{ye} = -\dfrac{C_f}{m}\tan^{-1}\left(\dfrac{\dfrac{v_{ye} + a\omega_e}{v_x}}{1+\left(\dfrac{v_y + a\omega_e}{v_x}\right)\left(\dfrac{v_{yd} + a\omega_d}{v_x}\right)}\right) - \dfrac{C_r}{m}\tan^{-1}\left(\dfrac{\dfrac{v_{ye} - b\omega}{v_x}}{1+\left(\dfrac{v_y - b\omega}{v_x}\right)\left(\dfrac{v_{yd} - b\omega_d}{v_x}\right)}\right) - v_x\omega_e + \dfrac{C_f}{m}\delta_{fe} \\ \dot{\omega}_e = -\dfrac{aC_f}{I_z}\tan^{-1}\left(\dfrac{\dfrac{v_y + a\omega}{v_x}}{1+\left(\dfrac{v_y + a\omega}{v_x}\right)\left(\dfrac{v_{yd} + a\omega_d}{v_x}\right)}\right) + \dfrac{bC_r}{I_z}\tan^{-1}\left(\dfrac{\dfrac{v_{ye} - b\omega}{v_x}}{1+\left(\dfrac{v_y - b\omega}{v_x}\right)\left(\dfrac{v_{yd} - b\omega_d}{v_x}\right)}\right) + \dfrac{aC_f}{I_z}\delta_{fe} \\ \ddot{e}_y = \dot{v}_{ye} + v_x\omega_e \end{cases} \tag{11}$$

From Eq. (11), it can be seen that the error quantity is still coupled with the reference quantity. In order to decouple the error quantity from the reference quantity, the virtual control rate is defined:

$$\bar{\delta}_{fe} = \delta_{fe} - \tan^{-1}\left(\dfrac{\dfrac{v_{ye} + a\omega_e}{v_x}}{1+\left(\dfrac{v_y + a\omega_e}{v_x}\right)\left(\dfrac{v_{yd} + a\omega_d}{v_x}\right)}\right) \tag{12}$$

Bringing Eq.(12) into Eq. (11) can be obtained:

$$\begin{cases} \dot{v}_{ye} = -\dfrac{C_r}{m}\tan^{-1}\left(\dfrac{\dfrac{v_{ye}-b\omega}{v_x}}{1+\left(\dfrac{v_y-b\omega}{v_x}\right)\left(\dfrac{v_{yd}-b\omega_d}{v_x}\right)}\right) - v_x\omega_e + \dfrac{C_f}{m}\bar{\delta}_{fe} \\ \dot{\omega}_e = \dfrac{bC_r}{I_z}\tan^{-1}\left(\dfrac{\dfrac{v_{ye}-b\omega}{v_x}}{1+\left(\dfrac{v_y-b\omega}{v_x}\right)\left(\dfrac{v_{yd}-b\omega_d}{v_x}\right)}\right) + \dfrac{aC_f}{I_z}\bar{\delta}_{fe} \\ \ddot{e}_y = \dot{v}_{ye} + v_x\omega_e \end{cases} \tag{13}$$

In conjunction with the design goals of the controller and the error dynamics equations, at the system equilibrium point e=0, the system dynamics Eq. (10) can be mapped to the error dynamics model (13). When (v_{ye}, ω_e) is chosen for the state variables, when $e = 0$ holds, for $\dot{e} = \ddot{e} = 0$ to also hold, the following equation must be guaranteed to hold:

$$-\frac{C_r}{m}\tan^{-1}\left(\frac{\dfrac{v_{ye}-b\omega}{v_x}}{1+\left(\dfrac{v_y-b\omega}{v_x}\right)\left(\dfrac{v_{yd}-b\omega_d}{v_x}\right)}\right) + \frac{C_f}{m}\bar{\delta}_{fe} = 0 \tag{14}$$

This moment:

$$\bar{\delta}_{fe} = \frac{C_r}{C_f}\tan^{-1}\left(\frac{\dfrac{v_{ye}-b\omega}{v_x}}{1+\left(\dfrac{v_y-b\omega}{v_x}\right)\left(\dfrac{v_{yd}-b\omega_d}{v_x}\right)}\right) \tag{15}$$

The virtual control rate of Eq. (15) can be obtained by realising the reduced order of Eq. (13):

$$\begin{cases} \dot{v}_{ye} = -v_x\omega_e \\ \dot{\omega}_e = \dfrac{(a+b)C_r}{I_z}\tan^{-1}\left(\dfrac{\dfrac{v_{ye}-b\omega}{v_x}}{1+\left(\dfrac{v_y-b\omega}{v_x}\right)\left(\dfrac{v_{yd}-b\omega_d}{v_x}\right)}\right) \end{cases} \tag{16}$$

The stability based on the closed-loop system dynamics Eq. (16) will be demonstrated in the following.

Theorem 1: The closed-loop system dynamics Eq. (16) is globally asymptotically stable at the equilibrium point.

Prove Theorem 1 below, choose the following Lyapunov function:

$$V_1 = \frac{1}{2}o_1 v_{ye}^2 + \frac{1}{2}o_2\omega_e^2 \tag{17}$$

where o_1 and o_2 are two constants greater than zero.

The first order derivative of V_1 with respect to time is:

$$\dot{V}_1 = -o_1 v_{ye} v_x \omega_e + o_2 \frac{(a+b)C_r}{I_z} \omega_e \tan^{-1}\left(\frac{\frac{v_{ye} - b\omega_e}{v_x}}{1 + \left(\frac{v_y - b\omega}{v_x}\right)\left(\frac{v_{yd} - b\omega_d}{v_x}\right)} \right) \tag{18}$$

For ease of presentation, let: $\chi_1 = o_2 \frac{(a+b)C_r}{I_z}$, $\chi_2 = \frac{v_{ye} - b\omega_e}{v_x}$, $\chi_3 = \omega_e$, $\chi_4 = \frac{v_{yd} - b\omega_d}{v_x}$, Eq. (17) can be simplified to:

$$\dot{V}_1 = -o_1 b v_x \chi_3^2 + \underbrace{\chi_3 \left(-o_1 v_x^2 \chi_2 + \chi_1 \tan^{-1}\left(\frac{\chi_2}{1 + \chi_4 \chi_2 + \chi_4^2} \right) \right)}_{\chi} \tag{19}$$

Since $-\frac{\pi}{2} \leq tan^{-1}(\bullet) \leq \frac{\pi}{2}$, Eq. (18) can be further converted to:

$$\dot{V}_1 \leq -o_1 b v_x \chi_3^2 + \chi_3 \left(-o_1 v_x^2 \chi_2 + \frac{\pi}{2} \chi_1 \right) = -o_1 b v_x \left(\chi_3 - \frac{\frac{\pi}{2}\chi_1 - o_1 v_x^2 \chi_2}{o_1 b v_x} \right)^2 + \frac{\left(\frac{\pi}{2}\chi_1 - o_1 v_x^2 \chi_2 \right)^2}{4 o_1 b v_x} \tag{20}$$

For Eq. (20), by choosing reasonable o_1 and o_2 one can make $2o_1 b v_x \chi_3 + 3o_1 v_x^2 \chi_2 > \frac{3\pi}{2} \chi_1$, which in turn makes $\dot{V}_1 < 0$.

Theorem 1 is proved.

4. Simulation Validation

In order to verify the effectiveness of the proposed trajectory tracking controller, the simulation model is built in MATLAB/Simulink and simulated in three simulation scenarios. The vehicle parameters used in the simulation process are shown in Table 1.

Table 1. Simulation parameters

Symbols	Values	Units
m	1530	kg
a	1.139	m
b	1.637	m
I_z	4607.47	kg/m^2
C_f	180000	N/rad
C_r	140000	N/rad

To verify the effectiveness of the S&T control method, the trajectory tracking performance of the proposed trajectory tracking controller and the LQR controller are compared in the lane changing scenario. During the simulation, the vehicle speed is 20m/s, the road surface attachment coefficient is 0.8, and the LQR controller is designed in reference [31]. The simulation results are shown in Figs.3-5, where Fig.3 shows the comparison curves of lateral displacement and lateral displacement error for trajectory tracking, Fig. 4 shows the comparison curves of yaw velocity and lateral velocity, and Fig.5 shows the comparison curves of front wheel angle calculated by the controller.

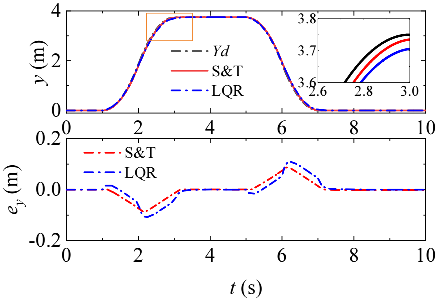

Figure 3. Lateral displacement and lateral displacement error

From Fig.3, it can be seen that both the LQR controller and the S&T control proposed in this paper can perform the tracking of the overtaking trajectory well. The maximum lateral displacement error is 0.11 m and the standard deviation (SD) of the lateral displacement error is 0.03 m when controlled by the LQR controller, and 0.09 m and 0.04 m when controlled by the S&T controller. In addition, the from the lateral displacement comparison curve, it can be seen that the S&T controller can track the reference trajectory faster. The comparison reveals that the trajectory tracking accuracy and convergence speed of the S&T controller is better than that of the LQR controller.

From Fig.3, it can be seen that both the LQR controller and the S&T control proposed in this paper can perform the tracking of the overtaking trajectory well. The maximum lateral displacement error is 0.11 m and the standard deviation (SD) of the lateral displacement error is 0.03 m when controlled by the LQR controller, and 0.09 m and 0.04 m when controlled by the S&T controller. In addition, the from the lateral displacement comparison curve, it can be seen that the S&T controller can track the reference trajectory faster. The comparison reveals that the trajectory tracking accuracy and convergence speed of the S&T controller is better than that of the LQR controller.

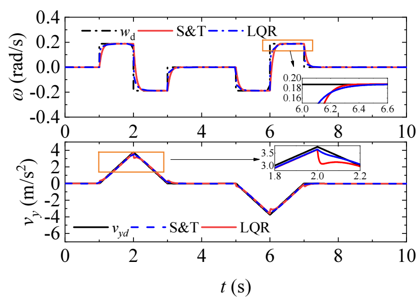

Figure 4. Yaw rate and lateral velocity

From Fig.4, it can be seen that the transverse pendulum angle and lateral velocity can track the ideal transverse pendulum angular velocity and ideal lateral velocity well when controlled by the S&T controller, and the convergence speed is fast. However, compared with the S&T controller, the LQR controller control process has a small amplitude of fluctuation, and the error is larger, and the convergence speed is slow.

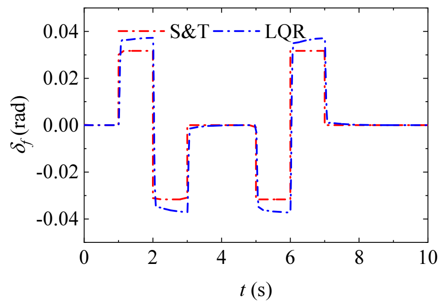

Figure 5. Front wheel angle calculated by controller

From Fig.5, it can be seen that in the steering process, the front wheel angle calculated by the LQR controller is larger than that of the S&T controller, and in the process of constant curvature, the size of the angle appears to increase gradually.

Comprehensively, it is easy to found that compared with the LQR controller, the designed S&T controller has better trajectory tracking accuracy, fast convergence speed, and can ensure the lateral stability of the vehicle while improving the trajectory tracking accuracy.

5. Conclusion

To improve the reliability and robustness of the trajectory tracking algorithm, this paper proposes a trajectory tracking controller based on the error dynamics model, which consists of two parts: the steady-state control rate and the transient control rate. The effectiveness of the method is verified by simulation, and the results show that the designed controller has high control accuracy and fast convergence speed. Compared with LQR, this trajectory tracking controller reduces the maximum lateral displacement error by 18.18% in lane changing scenarios and can track the reference trajectory faster.

References

[1] Wang H, Hu C, Zhou J, et al. Path tracking control of an autonomous vehicle with model-free adaptive dynamic programming and RBF neural network disturbance compensation[J]. Proceedings of the Institution of Mechanical Engineers, Part D: Journal of Automobile Engineering, 2022, 236(5): 825-841

[2] Spielberg N, Brown M, Kapania N, et al. Neural network vehicle models for high-performance automated driving[J]. Science Robotics, 2019, 4(28):1-13

[3] Yao W, Pang Z, Chi R, et al. Track tracking control of sanitation vehicle based on model-free adaptive iterative learning control[J]. Control Theory & Applications, 2022, 39(1): 101-108

[4] Wan N, Zeng G, Zhang C, et al. Multi-layer controller with state-constraint: Vehicle lateral stability control based on fuzzy logic[J]. Proceedings of the Institution of Mechanical Engineers, Part D: Journal of Automobile Engineering, 2022, 236(1): 155-167

[5] Hu Z, Huang J, Yang Z, et al. Cooperative-game-theoretic optimal robust path tracking control for autonomous vehicles[J]. Journal of Vibration and Control, 2022, 28(5-6): 520-535

[6] Wang Z, Zhou X, Wang J. Extremum-seeking-based adaptive model-free control and its application to automated vehicle path tracking[J]. IEEE/ASME Transactions on Mechatronics, 2022, (2): 1-11

[7] Jiang Y, Xu X, Zhang L, et al. Model free predictive path tracking control of variable-configuration unmanned ground vehicle[J]. ISA transactions, 2022, 123: 1-10

[8] Kd A, Sf A, Clpca B. Reinforcement learning based model-free optimized trajectory tracking strategy design for an AUV[J]. Neurocomputing, 2022, 469:289-297
[9] Elbanhawi M, Simic M, Jazar R, et al. Receding horizon lateral vehicle control for pure pursuit path tracking[J]. Journal of Vibration & Control, 2016, 24(3): 619-642
[10] Sun X, Wang Y, Hu W, et al. Path tracking control strategy for the intelligent vehicle considering tire nonlinear cornering characteristics in the PWA form[J]. Journal of the Franklin Institute, 2022, 359(6): 2487-2513
[11] Qing D, JI X, LIU Y, et al. Robust LPV/H∞ control for automatic path tracking of heavy commercial vehicles[J]. Journal of Tsinghua University (Science and Technology), 2022, 62(3): 438-446
[12] Zhang R, Xie Z, Zhao J, et al. Vehicle Path Following Control Method Based on MPC-NPLT[J]. Automobile Technology, 2022(3): 28-34
[13] Lin F, Chen Y, Zhao Y, et al. Path tracking of autonomous vehicle based on adaptive model predictive control[J]. International Journal of Advanced Robotic Systems, 2019, 16(5):1-12
[14] Wu H, Si Z. Intelligent vehicle trajectory tracking control based on linear matrix inequality[J]. Journal of Zhejiang University(Engineering Science) , 2020, 54(1): 110-117
[15] Zhao Y, Wang J, Ji X, et al. Path Tracking for Evasive Collision Avoidance Based on Active Disturbance Rejection Control[J]. Journal of Tongji University(Natural Science) , 2015, 43(8): 1200-1204
[16] Sánchez I, D'Jorge A, Raffo G V, et al. Nonlinear model predictive path following controller with obstacle avoidance[J]. Journal of Intelligent & Robotic Systems, 2021, 102(1): 1-18
[17] Cheng S, Li L, Chen X, et al. Model-predictive-control-based path tracking controller of autonomous vehicle considering parametric uncertainties and velocity-varying[J]. IEEE Transactions on Industrial Electronics, 2020, 68(9): 8698-8707
[18] Yu S, Li X, Chen H, et al. Nonlinear model predictive control for path following problems[J]. International Journal of Robust and Nonlinear Control, 2015, 25(8): 1168-1182
[19] Song R, Ye Z, Wang L, et al. Autonomous Wheel Loader Trajectory Tracking Control Using LPV-MPC[J]. arXiv e-prints, 2022, 2203.08944:1-11
[20] Li L, Li J, Zhang S. Trajectory tracking control of autonomous vehicles with optimized sliding mode control[J]. Journal Of Automotive Safety and Energy, 2020,11(4):503-510
[21] Yin C, Wang S, Li X, et al. Trajectory tracking based on adaptive sliding mode control for agricultural tractor[J]. IEEE Access, 2020, 8: 113021-113029
[22] Park B S, Yoo S J, Park J B, et al. Adaptive neural sliding mode control of nonholonomic wheeled mobile robots with model uncertainty[J]. IEEE Transactions on Control Systems Technology, 2008, 17(1): 207-214
[23] Binh N T, Tung N A, Nam D P, et al. An adaptive backstepping trajectory tracking control of a tractor trailer wheeled mobile robot[J]. International Journal of Control, Automation and Systems, 2019, 17(2): 465-473
[24] Wang S, Bao X, Zhang S, et al. Trajectory Tracking Control of Wheeled Mobile Robots Using Backstepping[C]//International Conference on Intelligent Robotics and Applications. Springer, Cham, 2019: 289-300
[25] Hwang C, Yang C, Hung J. Path tracking of an autonomous ground vehicle with different payloads by hierarchical improved fuzzy dynamic sliding-mode control[J]. IEEE Transactions on Fuzzy Systems, 2017, 26(2): 899-914
[26] Yu R, Ding S, Tian H, et al. A hierarchical constraint approach for dynamic modeling and trajectory tracking control of a mobile robot[J]. Journal of Vibration and Control, 2021, 28(5-6):564-576
[27] Yin H, Chen Y-H, Huang J, et al. Tackling mismatched uncertainty in robust constraint-following control of underactuated systems[J]. Information Sciences, 2020, 520:337-352
[28] Pacejka H B, Besselink I. Magic Formula Tyre Model with Transient Properties[J]. Vehicle System Dynamics, 1996, 27:234-249
[29] Satouri M R, Marashian A, Razminia A. Trajectory tracking of an autonomous vehicle using immersion and invariance control. 2021, 358(17): 8969-8992
[30] Kokotovic P, Marino R. On vanishing stability regions in nonlinear systems with high-gain feedback.[J]. IEEE Transactions on Automatic Control, 2003, 31(10):967-970
[31] Hu J, Zhong X, Chen R, et al. Path Tracking Control of Intelligent Vehicles Based on Fuzzy LQR[J]. Automotive Engineering. 2022,44(1):17-25,43